A user-friendly two-color super-resolution localization microscope

Teng Zhao,[1] Ying Wang,[1] Yuanliang Zhai,[2] Xiaoxuan Qu,[2] Aifang Cheng,[2] Shengwang Du[1] and M. M. T. Loy[1,*]

[1]*Department of Physics, The Hong Kong University of Science and Technology, Hong Kong, China*
[2]*Division of Life Science, The Hong Kong University of Science and Technology, Hong Kong, China*
[*]*phloy@ust.hk*

Abstract: We report a robust two-color method for super-resolution localization microscopy. Two-dye combination of Alexa647 and Alexa750 in an imaging buffer containing COT and using TCEP as switching regent provides matched and balanced switching characteristics for both dyes, allowing simultaneous capture of both on a single camera. Active sample locking stabilizes sample with 1nm accuracy during imaging. With over 4,000 photons emitted from both dyes, two-color superresolution images with high-quality were obtained in a wide range of samples including cell cultures, tissue sections and yeast cells.

OCIS codes: (110.0180) Microscopy; (180.2520) Fluorescence microscopy; (100.6640) Superresolution.

References and links

1. M. J. Rust, M. Bates, and X. Zhuang, "Sub-diffraction-limit imaging by stochastic optical reconstruction microscopy (STORM)," Nat. Methods **3**(10), 793–796 (2006).
2. E. Betzig, G. H. Patterson, R. Sougrat, O. W. Lindwasser, S. Olenych, J. S. Bonifacino, M. W. Davidson, J. Lippincott-Schwartz, and H. F. Hess, "Imaging Intracellular Fluorescent Proteins at Nanometer Resolution," Science **313**(5793), 1642–1645 (2006).
3. S. T. Hess, T. P. K. Girirajan, and M. D. Mason, "Ultra-High Resolution Imaging by Fluorescence Photoactivation Localization Microscopy," Biophys. J. **91**(11), 4258–4272 (2006).
4. M. Bates, B. Huang, G. T. Dempsey, and X. Zhuang, "Multicolor Super-Resolution Imaging with Photo-Switchable Fluorescent Probes," Science **317**(5845), 1749–1753 (2007).
5. G. T. Dempsey, J. C. Vaughan, K. H. Chen, M. Bates, and X. Zhuang, "Evaluation of fluorophores for optimal performance in localization-based super-resolution imaging," Nat. Methods **8**(12), 1027–1036 (2011).
6. H. Shroff, C. G. Galbraith, J. A. Galbraith, H. White, J. Gillette, S. Olenych, M. W. Davidson, and E. Betzig, "Dual-color superresolution imaging of genetically expressed probes within individual adhesion complexes," Proc. Natl. Acad. Sci. U.S.A. **104**(51), 20308–20313 (2007).
7. M. Heilemann, S. van de Linde, M. Schüttpelz, R. Kasper, B. Seefeldt, A. Mukherjee, P. Tinnefeld, and M. Sauer, "Subdiffraction-Resolution Fluorescence Imaging with Conventional Fluorescent Probes," Angew. Chem. Int. Ed. Engl. **47**(33), 6172–6176 (2008).
8. J. Tam, G. A. Cordier, J. S. Borbely, Á. Sandoval Álvarez, and M. Lakadamyali, "Cross-Talk-Free Multi-Color STORM Imaging Using a Single Fluorophore," PLoS ONE **9**(7), e101772 (2014).
9. R. Jungmann, M. S. Avendaño, J. B. Woehrstein, M. Dai, W. M. Shih, and P. Yin, "Multiplexed 3D cellular super-resolution imaging with DNA-PAINT and Exchange-PAINT," Nat. Methods **11**(3), 313–318 (2014).
10. I. Testa, C. A. Wurm, R. Medda, E. Rothermel, C. von Middendorf, J. Fölling, S. Jakobs, A. Schönle, S. W. Hell, and C. Eggeling, "Multicolor Fluorescence Nanoscopy in Fixed and Living Cells by Exciting Conventional Fluorophores with a Single Wavelength," Biophys. J. **99**(8), 2686–2694 (2010).
11. J. Tang, J. Akerboom, A. Vaziri, L. L. Looger, and C. V. Shank, "Near-isotropic 3D optical nanoscopy with photon-limited chromophores," Proc. Natl. Acad. Sci. U.S.A. **107**(22), 10068–10073 (2010).
12. M. Bates, G. T. Dempsey, K. H. Chen, and X. Zhuang, "Multicolor Super-Resolution Fluorescence Imaging via Multi-Parameter Fluorophore Detection," ChemPhysChem **13**(1), 99–107 (2012).
13. J. C. Vaughan, G. T. Dempsey, E. Sun, and X. Zhuang, "Phosphine Quenching of Cyanine Dyes as a Versatile Tool for Fluorescence Microscopy," J. Am. Chem. Soc. **135**(4), 1197–1200 (2013).
14. N. Olivier, D. Keller, P. Gönczy, and S. Manley, "Resolution Doubling In 3D-STORM Imaging through Improved Buffers," PLoS ONE **8**(7), e69004 (2013).
15. B. K. P. Horn, "Closed-form solution of absolute orientation using unit quaternions," J. Opt. Soc. Am. A **4**(4), 629–642 (1987).
16. R. McGorty, D. Kamiyama, and B. Huang, "Active microscope stabilization in three dimensions using image correlation," Opt .Nanoscopy **2**(1), 3 (2013).

#230521 - $15.00 USD Received 11 Dec 2014; revised 13 Jan 2015; accepted 13 Jan 2015; published 23 Jan 2015

17. P. K. Koo, S. U. Setru, and S. G. J. Mochrie, "Active drift stabilization in three dimensions via image cross-correlation," Rev. Sci. Instrum. **84**(10), 103705 (2013).
18. A. Dani, B. Huang, J. Bergan, C. Dulac, and X. Zhuang, "Superresolution Imaging of Chemical Synapses in the Brain," Neuron **68**(5), 843–856 (2010).
19. J. Ries, C. Kaplan, E. Platonova, H. Eghlidi, and H. Ewers, "A simple, versatile method for GFP-based super-resolution microscopy via nanobodies," Nat. Methods **9**(6), 582–584 (2012).

1. Introduction

The invention and development of super-resolution localization microscopy [1–3] enables optical fluorescence imaging down to nanometer scale. The basic elements of the technique are: first, the ability to detect single fluorophores and localize with high precision, and second, some schemes to arrange for multiple, sparse subsets of non-overlapping probes to emit and be localized. The sum of these localized subsets then presents a super-resolved image of the overlapping probes on the underlying structure. Such ability to visualize intracellular organelles below the Abby limit of 200nm is particularly attractive to researchers in the field of life science.

Of crucial importance to biologists is the ability to image in two or more colors to study co-localization of proteins and structures. Multi-color localization microscopy has been realized in a number of approaches including (1) using switchable dye-pairs with either distinct activators or distinct reporters [4], (2) using different photoactivable fluorescent proteins or dye molecules with separable excitation and emission spectrum [5–7], and (3) the use of single fluorophore by sequential labeling [8, 9]. All these methods have been successfully demonstrated, albeit with various caveats of possible crosstalk, unbalanced localization accuracies in different colors, or prolonged imaging time. Special constructs of dye-pairs are also required in some of these methods.

We present here a user-friendly two-color superresolution system using commercial dyes applicable to wide range of biological applications. For biological imaging, it is highly desirable that: (1) the laser excitation power be low in order to minimize the adverse effect of photo-toxicity and bleaching, and (2) both color channels should be simultaneously recorded rather than imaged sequentially [10, 11]. This split-channel type detection is twice as fast. More importantly the two-color alignment can be robust with the use of geometrically fixed filter sets Once calibrated and stored, high resolution two-color images with good registration can be obtained without further user action.

Since the two channels are captured on different parts of the same camera frame, it is essential that the two dyes used must be well balanced in terms of photon counts, bright (on) time as well as similarly low on/off ratios. It is also critical to control and compensate for any drift between the microscope objective and the sample stage, which if left uncontrolled can amount to hundreds of nanometers over a time period of minutes in a typical laboratory environment.

2. Enhanced photo-switching of Alexa647 and Alexa750 in TCEP + COT imaging buffer

Vaughan et al. reported that TCEP (phosphine tris(2-carboxyethyl)phosphine) can control the photoswitching behavior of both Alexa647 and Alexa750 to have almost equal amount of photon emission [12, 13]. Thus, they suggested that these two dyes are particularly attractive for two-color imaging, which we adopt as our choice. However, the use of TCEP has the undesirable effect of reducing the photon counts such that for high resolution imaging, a rather high dose of laser excitation is required, potentially leading to photo-toxicity and bleaching. For this combination to be generally usable, this shortcoming will need to be remedied, with the necessary condition that both dyes must respond similarly to retain the advantage of nearly equal photon counts. We reasoned that this might be possible, since TCEP controls the switching dynamic by the formation of a covalent adduct resulting in the dark state. In between adduct formation, the dye emit photons while in the singlet state but not in the triplet state. Addition of a triplet quencher such as COT (cyclooctatetraene) should minimize the time in triplet state and thus increase photon count without changing the switching dynamic [14].

#230521 - $15.00 USD Received 11 Dec 2014; revised 13 Jan 2015; accepted 13 Jan 2015; published 23 Jan 2015

To characterize the dye molecule behaviors in TCEP imaging buffer with COT, we made single molecule samples by conjugating Alexa647 and Alexa750 to different antibodies with low ratio (1:6) so that in most case for each antibody there is at most one dye. The antibodies are immobilized on a poly-lysine coated coverslip, and continuously illuminated by 4kW/cm^2 656nm laser for Alexa647 or 4.5kW/cm^2 750nm laser for Alexa750. To study the photoswitching behavior, the fluorescence signal traces of each molecule in different buffers conditions are recorded, and the photon emission of each switching cycle, and the duration of each emission period (τ_{on}) is measured.

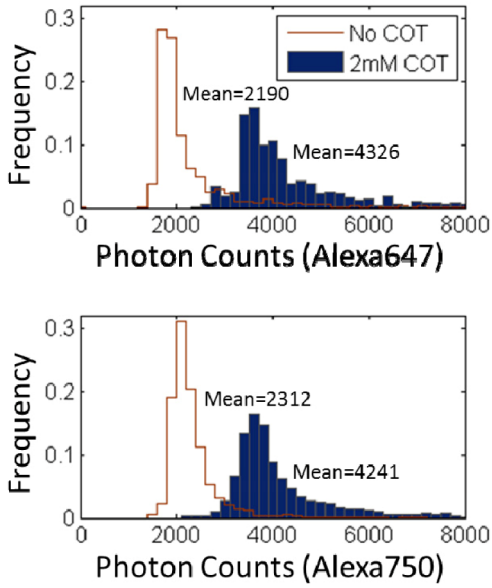

Fig. 1. The photon counts distribution of Alexa647 and Alexa750 in TCEP only buffer and TCEP + COT buffer. TCEP + COT buffer doubles the photon emission during photoswitching while keeping a good balance between the two dyes. Data measured under the excitation power of 4kW/cm^2 for 656nm laser and 4.5kW/cm^2 for 750nm laser.

We found that by introducing 2mM of COT into 50mM TCEP imaging buffer (TCEP + COT buffer), photon counts of over 4,000 are observed in both dyes, twice the number when no COT is added, as shown in Fig. 1. Particularly noteworthy is that the excitation laser intensities required are some five times *lower* than values reported by Vaughan et al. [13], allowing longer duration imaging time before photobleaching sets in.

In addition to the well-balanced photon counts between the dyes, a good match of photoswitching cycles are also observed with above conditions. As shown in Fig. 2, both fluorophores are found having almost identical on time (τ_{on}) with the majority of on times being close to 30ms. This characteristic enables simultaneous effective detection of both dyes on the same camera frame with the same exposure time.

The on/off ratios of Alexa647 and Alexa750 in TCEP + COT buffer were measured to be ~0.0005 and ~0.0003, respectively, about the same values from TCEP only imaging buffer. This confirms our expectation that as a triplet state quencher (TSQ), COT acts effectively to keep the fluorophore from the non-emissive triplet state, and does not interference with the adduct induced dark state formation. Note that the on/off ratio in both TCEP + COT buffer and TCEP only buffer is significantly reduced compared with that in thiol buffer (~0.002 and ~0.0006 for Alexa647 and Alexa750), making this combination of dyes suitable also for densely labeled structures [5, 12].

#230521 - $15.00 USD Received 11 Dec 2014; revised 13 Jan 2015; accepted 13 Jan 2015; published 23 Jan 2015

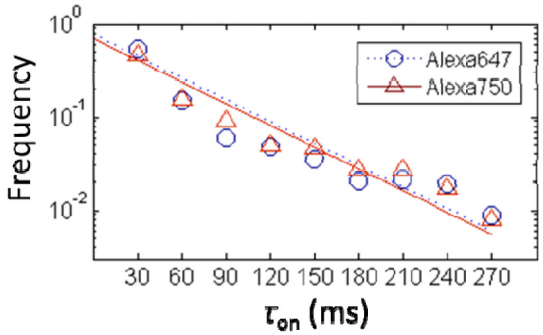

Fig. 2. The on-time distributions of Alexa647 and Alexa750 in optimized TCEP + COT imaging buffer show a good match between channels. Mean τ_{on} for Alexa647 and Alexa750 are 100ms and 108ms, respectively. Data measured under the excitation power of 4kW/cm^2 for 656nm laser and 4.5kW/cm^2 for 750nm laser.

The optimized TCEP + COT imaging buffer used in this paper contains 50mM TCEP, 2mM COT, 5U/ml pyranose oxidase, 10%(w/v) glucose, 57μg/ml catalase, 1mM ascorbic acid and 1mM methyl viologen dissolved in 200mM Tris-Cl with pH9.0. The TCEP concentration is higher than introduced by Vaughan et al. in order to achieve lower on/off ratio. We also followed the protocol using a combination of pyranose oxidase, glucose and catalase as oxygen scavenger to keep the pH stable during imaging [13, 14].

3. System setups

Our system is shown in Fig. 3. The excitation is provided by a 500mW 656nm DPSS laser (CNI) and a 500mW 750nm diode laser (LeadingTech). Both laser beams are combined and coupled into a fiber to filter out higher order modes. The laser output from the fiber is then focused at the back focal plane of a 100 × 1.4 N. A. infinite corrected objective (Nikon Apo TIRF) via a confocal geometry to provide total internal reflection (TIRF) type illumination at the sample. The sample is double stained with Alexa647 and Alexa750, and immersed in an approximately 300μL imaging buffer, held by a home-designed chamber. Fluorescent signal from the sample is collected by the objective, and focused by the first tube lens to form the intermediate image, which is then cropped by a rectangular mask. The two channels are separated by a short-pass dichroic mirror (Chroma ZT656/750rpc), forming images on the top and bottom half-areas of an EMCCD camera by the second tube lens. Emission filters (Chroma ET700/50m and ET810/90m) are placed in the path of each channel to further block the excitation laser as well as any channel crosstalk.

Accurate channel registration is performed to remove any chromatic aberrations in the final two-color image. To do so we conjugate both Alexa647 and Alexa750 dye onto the same IgG3 antibody with high dose. The antibody is frozen at −20°C overnight to form small aggregation, then deposited onto poly-lysine coated coverslips, and visualized under the fluorescent microscope. The aggregates with sizes under diffraction limit are visualized as bright dots on both channels. Typically 6 to 8 dots distributed across the whole field of view are chosen as landmarks for alignment and their absolute positions are determined to nanometer by Gaussian fitting. A 3 × 3 alignment matrix containing translation, rotation and rescaling is worked out using Horn's method [15] by matching the positions of these dots from the two channels. Once the alignment is done, the system can be operated for weeks to produce chromatic aberration free two color super-resolved images.

#230521 - $15.00 USD Received 11 Dec 2014; revised 13 Jan 2015; accepted 13 Jan 2015; published 23 Jan 2015

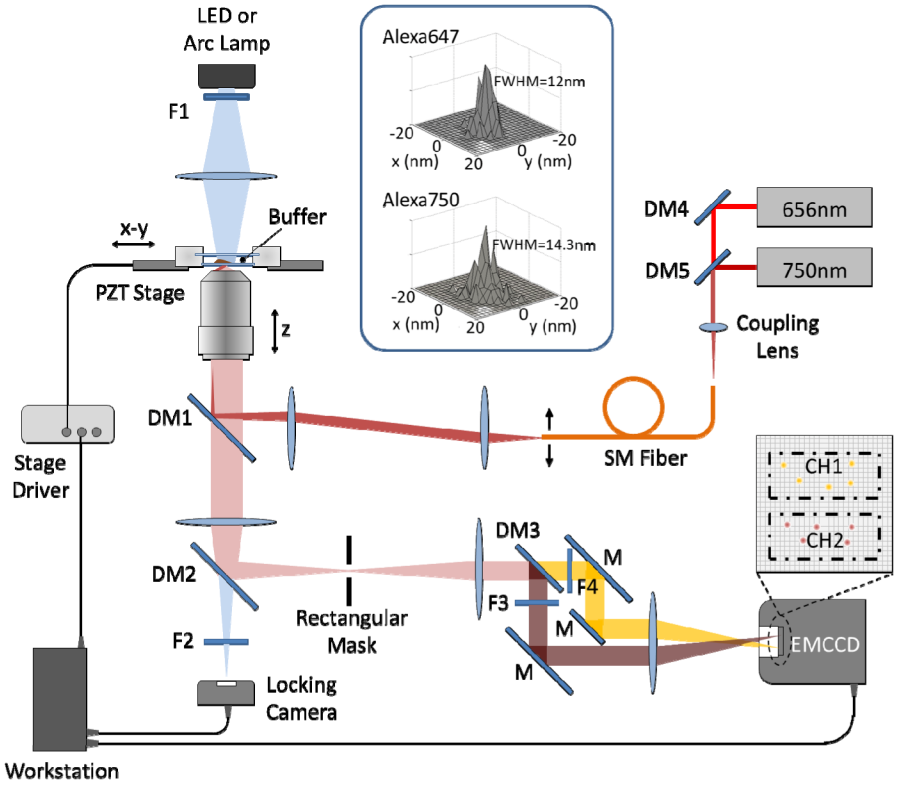

Fig. 3. The schematics of a two-color localization microscope with split-channel type detection path. DM1: multiband dichroic mirror (Chroma) that reflects excitation/activation lasers and transmits fluorescent signals. DM2: short pass dichroic mirror (Chroma) cut off at 650nm that reflects fluorescent signals and transmits the scattered image from sample. DM3 is a short pass dichroic mirror (Chroma) cut off at 755nm to split the two fluorescent channels. DM4 and DM5 are laser beam combiners (Thorlabs). M stands for mirrors. F1 and F2 are identical bandpass filters (Chroma) that block the laser and fluorescence from sample thus let locking camera only accept scattered image from sample. F3 and F4 are the emission filters (Chroma) for Alexa750 and Alexa647, respectively. The inset shows super resolution image profiles of Alexa647 and Alexa750 single molecules. The FWHM widths are under 15nm in both channels, consistent with $\delta = \mathrm{PSF}/\sqrt{N}$ where N is the photon number.

To have spatial resolution of 20nm, it is obvious that any sample drift must be kept well under that distance. For superresolution localization microscopy, this is particularly challenging since the super-resolved image is reconstructed from many thousands of frames, often taking minutes to capture, and any drift over this time scale will blurred the final reconstructed image. We adopt a method using a scattering image of the sample itself to lock the position with nanometer accuracy for extended period of time. As shown in Fig. 3, during data acquisition, in addition to the laser excitation, the sample is also illuminated by a LED or filtered arc lamp with wavelength shorter than 656nm so this locking channel can be isolated with any imaging channels. The cells form scattering images on a simple CMOS mega pixel camera (locking camera in Fig. 3). Using LabVIEW software, the Normalized cross-correlation (NCC) graph which represents the likelihood between the current image and the reference image [16, 17] is calculated from a cropped region of scatter image that has higher SNR. The motion of sample is detected by tracking the centroid of the NCC graph. Software then drives the PZT stage (Physik Instrumente M545) via a fine tuned proportional-integration-differentiator (PID) circuit to cancel out the movement in real time with 10Hz bandwidth determined by the frame rate of locking camera.

#230521 - $15.00 USD Received 11 Dec 2014; revised 13 Jan 2015; accepted 13 Jan 2015; published 23 Jan 2015

This active locking removes the x-y drift, and the PFS (Perfect Focus System) feature in our Nikon microscope actively stabilizes the sample to objective distance (z-axis). To evaluate the locking performance we deposited a sparse layer of 1.2μm polystyrene beads fixed on the coverslip, allowing us to measure any movement between the microscope objective and the sample stage. These beads generate strong scattering signal with SNR>10 allowing NCC tracking with high accuracy [17]. The sample movements without and with the active locking are then measured by tracking on one of the beads, as shown in Fig. 4. Results indicate that sample may drift nonlinearly over 200 nm over 15 minutes when locking is inactivated. With locking turned on, the sample can be stabilized at a position with STD = 1nm that is beyond the resolution of localization microscopy.

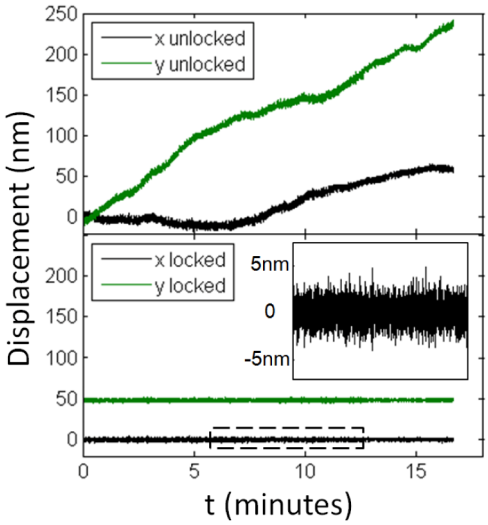

Fig. 4. The performance of active sample locking. NCC tracking of a 1.2μm polystyrene bead measures sample movement. The bead produces scattered imaging with SNR>10, allowing tracking with sub nanometer resolution. Insertion zooms in the marked area showing the locking is able to stabilize sample with nanometer resolution.

4. Measurement results

This two-color localization microscope has been used by biologists to image a variety of samples, including: (1) mitochondrial sub-organelle structure in mammalian cell cultures, (2) chemical synapse in brain tissue slices, and (3) microtubule-spindle complex in yeast cells.

4.1 Mitochondrial structure in HEK293 cell line

We resolved the mitochondrial structure in mammalian cells using our two-color set-up. Tom20 is a subunit of the mitochondrial import receptor complex on the outer membrane, while the p32 is a protein mainly localized in the mitochondrial matrix. We used a specific primary antibody of Tom20 and anti-rabbit Alexa647 antibody as the secondary antibody to label Tom20. An Alexa750-coupled primary antibody of p32 was applied to mark p32.

The sample was immersed in imaging buffer as described before, and isolated from air using a home-build imaging chamber. During imaging, the Epi-fluorescent images were taken prior to the super-resolution imaging, where low excitation intensities were used. TIRF illumination was carefully adjusted in the Epi mode. Once the desired area was located, the active sample locking was also initialized as described previously. Localization imaging was initialized by increasing excitation intensity to 4kW/cm^2 (656nm) and 4.5kW/cm^2 (750nm) so that blinking signals of molecules were separable. EMCCD recorded the blinking into a movie having 30,000 frames at 30Hz with a typical EM gain of 100. The total acquisition process takes ~15 minutes. Meanwhile localization software grabbed the images from

#230521 - $15.00 USD Received 11 Dec 2014; revised 13 Jan 2015; accepted 13 Jan 2015; published 23 Jan 2015

EMCCD, cropped out the region of each channel, and processed individually to get the localized position map on each channel. The positions on two channels were aligned together by the previous mentioned alignment matrix to form the final two-color super-resolution image.

We successfully resolved the mitochondrial structure where Tom20 marked outer membrane packs the matrix protein p32 with fitting error smaller than 15nm in both channels, as shown in Fig. 5.

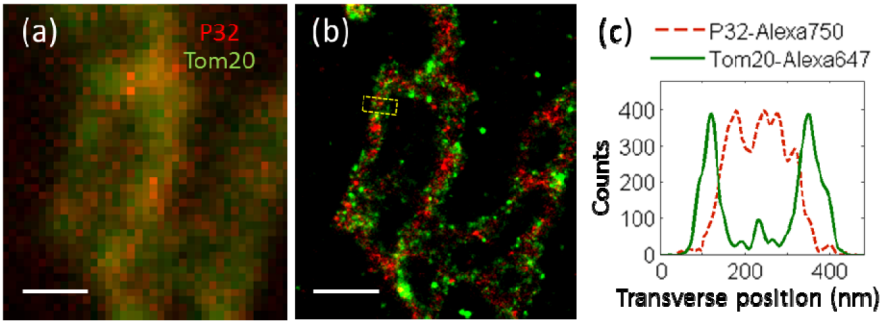

Fig. 5. Two-color super resolution imaging resolves p32 (mitochondrial matrix) packed by Tom20 (mitochondrial outer membrane) in HEK293 cell line. (a) Epi fluorescent image with totally blurred structure. (b) The super resolution images at the same location. (c) The transvers profile correspondence to boxed region in (b), showing clear the p32 is packed inside mitochondrial outer membrane. Scale bars: 1μm.

4.2 The synaptic components in brain slices

Imaging of tissue sample laid high requirement on microscopes compared to cultured cells due to the presence of strong background signal. The TIRF illumination must be perfectly aligned in order to remove background from out-of-focus structures. In addition the thickness of tissue increases scattering of fluorescent emission and reduces the dye brightness. Since Rayleigh scattering, the major scattering in tissue, has strong wavelength dependence (proportional to λ^{-4}), long-emission dye like Alexa647 and Alexa750 has unique advantage in this application. Besides, the high structure density in tissues also challenges localization microscopy. TCEP based imaging buffer counters the problem as it allows photo-switching with much lower on/off ratio thus guarantees accurate localization.

The brain of 129s mice strain was dissected and cryo-sectioned into 5um thick slices using optimal cutting temperature compound (OCT) embedding. In order to apply TIRF illumination to reduce background, the tissue was directly retrieved with gelatin coated coverslips so the surface of sample was in contact with glass. To image the synaptic architecture we stained two abundant scaffolding proteins, Bassoon of pre-synapse and Homer1 of post-synapse with Alexa647 and Alexa750, respectively. The imaging procedure was the same as introduced previously. As shown in Fig. 6, due to the diffraction limit, in Epi-fluorescent image the pre- and post- synaptic structure was totally unresolvable. With super-resolution image from localization microscopy, one could clearly visualize the Bassoon and Homer1 clusters flanking the synaptic cleft [18].

#230521 - $15.00 USD Received 11 Dec 2014; revised 13 Jan 2015; accepted 13 Jan 2015; published 23 Jan 2015

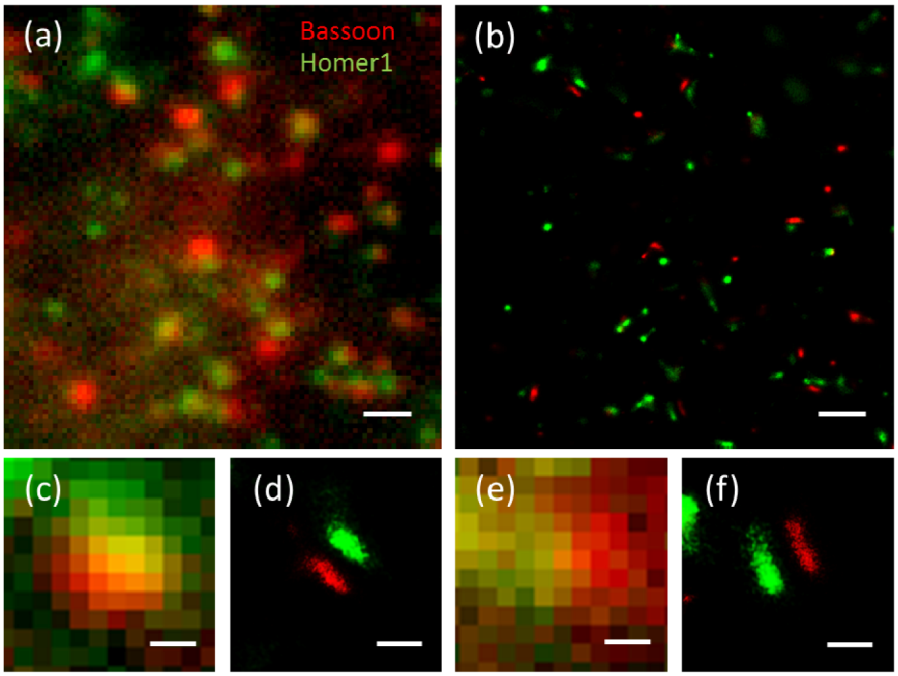

Fig. 6. Synaptic structure in tissue slice resolved by localization microscope. (a)(c) and (e) show the EPI-fluorescent image which fails to tell the details of structure. (b)(d) and (f) are superresolution images acquired by designed two-color localization microscope. The pre- and post-synaptic structures are clearly resolved. Scale bars: 1μm in (a) and (b); 200nm in (c) and (d).

4.3 Microtubule-spindle complex in yeast cells

Yeast cells are commonly very compact and small with strong scattering and auto-fluorescent background. The staining of yeast cells are challenging as well due to the cell wall normally impermeable to common antibody. Nanobody [19] having much smaller size could go through the cell wall but with limited efficiency. Also its low cross-link ratio (2 probes per nanobody) leads to weak fluorescent signal. Higher staining concentration can be used to increase labelling density however non-specific background will become strong. The low photon budget in our system minimizes the effect of photobleaching so that satisfying images can be obtained using nanobody even with low concentration of staining. Besides, autofluorescence is reduced by the long excitation wavelength and mild excitation intensity, while the low on/off ratio of the dyes in TCEP also helped with imaging of yeast organelles with high protein density.

#230521 - $15.00 USD Received 11 Dec 2014; revised 13 Jan 2015; accepted 13 Jan 2015; published 23 Jan 2015

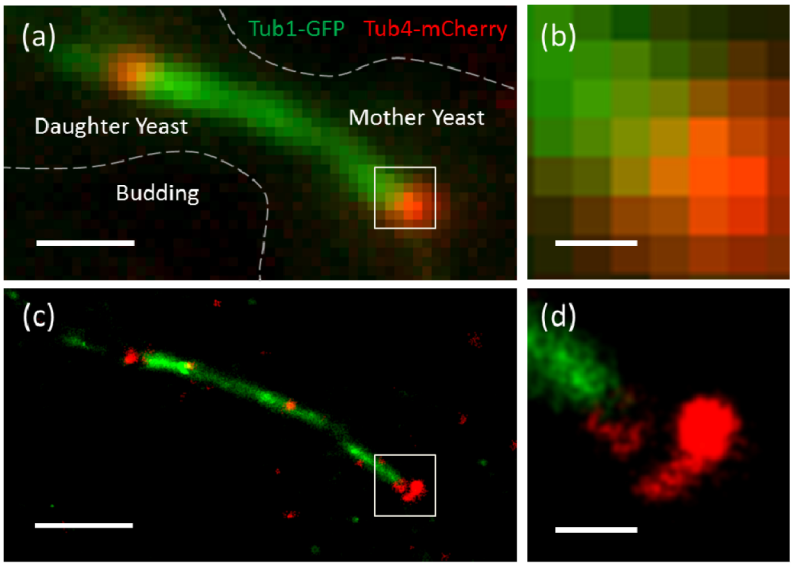

Fig. 7. Two-color super resolution imaging of Alexa750-anti-GFP nanobody labeled Tub1 of spindle microtubule and Alexa647-anti-RFP nanobody labeled Tub4 of spindle pole body in a yeast cell. (a) and (b) are Epi fluorescent images where (b) is the zoom in of the marked area in (a). (c) and (d) are the two-color super resolution images at the same position where the anchoring of spindle microtubules to spindle pole bodies can be clearly resolved. Scale bar: 1μm in (a) and (b); 200nm in (c) and (d).

To study the γ-tubulin complex-mediated anchoring of spindle microtubules to spindle-pole bodies (SPBs) in budding yeast, we used Alexa750-coupled anti-GFP and Alexa647-conjugated anti-RFP nanobodies to label α-tubulin GFP-Tub1 and γ-tubulin component Tub4-mCherry respectively. Two-color super-resolution images were obtained following the same imaging procedure. Without obvious effect of photobleaching and background, the anchoring of spindle microtubule bundles by γ-tubulin to spindle pole bodies during mitosis were visualized as shown in Fig. 7.

5. Conclusion

We designed and built a two-color localization microscope using two IR emitting flourphores: Alexa647 and Alexa750 in an imaging buffer containing TCEP to control photo switching, and COT as triplet state quencher to boost the photon emission of both dyes. With modest laser intensities below 5kW/cm^2, probes shall have low photobleaching rate, enabling sample staining with lower concentration to reduce non-specific background. Spatial resolution of 20nm can be routinely obtained for both channels. With the split-screen configuration and all the filters in fixed geometry, chromatic aberration between the two channels can be easily corrected. Active sample tracking allows operation in ordinary laboratory environment with no special requirements for temperature control or ground floor vibration-free requirements. This system has been intensively used by life science researchers and has proven to be easy-to-use with stable performance.

Acknowledgments

We acknowledge Kenny K. K. Chung and Karl Herrup for their instructions in sample preparation. We also thank Wei Jin for his help in yeast sample preparation and imaging. This work was supported by a grant from the Offices of the Provost, VPRG and Dean of Science, HKUST (HKUST VPRGO12SC02), and Hong Kong Research Grants Council (HKUST12/CRF/13G). The work was also partially supported by NanoBioImaging Ltd. through a research contract with HKUST R and D Corporation Ltd (RDC 13142150).

#230521 - $15.00 USD Received 11 Dec 2014; revised 13 Jan 2015; accepted 13 Jan 2015; published 23 Jan 2015